Vibrato of saxophones

Joël Gilbert, Jonathan Terroir, Laurent Simon

Vibrato of saxophones

J. Gilbert, L. Simon(*) and J. Terroir

Laboratoire d'Acoustique de l'Université du Maine, UMR-CNRS 6613, Université du Maine, Avenue Olivier Messiaen 72085 Le Mans Cedex 09, France.

Received

running title : Vibrato of saxophones

(*) Corresponding author, laurent.simon@univ-lemans.fr

Abstract

Several alto saxophone players' vibratos have been recorded. The signals are analysed using time-frequency methods in order to estimate the frequency modulation (vibrato rate) and the amplitude modulation (vibrato extent) of each vibrato sample. Some parameters are derived from the results in order to separate the two ways of vibrato playing : vibrato "à la machoire" and vibrato "sur l'air". Moreover, time domain simulations of single-reed instruments vibratos are created. The model is controlled by two parameters : the mouth overpressure and a parameter characterizing the reed-mouthpiece system. Preliminary comments and comparisons between the simulated vibratos and recorded vibratos results are done.

PACS numbers :

I. INTRODUCTION

Vibrato is one of the common ornaments in occidental classical music, particularly in singing, but in wind and bowed instruments too. When the instruments are played using vibrato ornaments, deliberate fluctuations in the period and the amplitude of the acoustic pressure signals are applied.

Most of the studies dedicated to vibrato have been concerned with lyric singers[1,2,3,4,5] trying to measure the properties like the vibrato rate (frequency modulation) or the vibrato extent (amplitude modulation), and then to analyse the vibrato structure along time, or to study their pitch perception. Our study is devoted to the single reed wind instruments and particularly to the alto saxophone. Following Christophe Bois (a french professional saxophone player), there are many kinds of vibratos which can be separated in two sets according to the way they are produced : (1) the vibratos "à la machoire " (the vibrato effect comes from a slight mechanical vibration of the jaw), (2) the vibratos "sur l'air " (the vibrato effect comes from a slight modulation of the mouth cavity air pressure controlled by the tongue). First, the aim of the study is to analyse different stable vibratos, by extracting their amplitude modulation and frequency modulation parameters, one question being, is it possible to separate the two kinds of vibratos by analysing the corresponding generated sounds ? Secondly, some simulated vibratos based on the physical modelling of an idealized saxophone are analysed too.

The present paper is divided in four sections. After this brief introduction, the methods to extract the parameters of the amplitude modulation and of the frequency modulation are presented in section II. Then the methods are checked on known test signals in order to estimate accuracies, then applied to alto saxophone players' vibratos and applied to simulated vibratos in section III. Finally, the preliminary conclusions and the perspectives of this work are discussed in the conclusion, section IV.

II. SIGNAL PROCESSING METHODS

Vibrato in permanent regime may be modelled as both an amplitude modulation and a frequency modulation of a signal. Estimating both modulations allows then to extract parameters of modeling. For amplitude modulation, we show that estimations based on methods such as envelop detection are accurate enough. For frequency modulation, time-frequency analysis is required. Several time-frequency methods (spectrogram[1,2], modal distribution[6]) were used in other vibrato studies. In the paper, we use the spectrogram and the instantaneous frequency is estimated as the local frequency of the spectrogram[7].

A. Modelling of test signal

For most of musical signals, the signal $s(t)$ is modelled as a discrete sum of partials[6], i.e.

$$s(t) = \sum_{n=1}^{N_h} a_n(t) \cos(\phi_n(t)), \tag{1}$$

where $a_n(t)$ is the amplitude modulation and $\phi_n(t)$ is the instantaneous phase of the n-th partial, respectively, and where N_h is the number of harmonics of the playing frequency. It is furthermore supposed that $a_n(t)\cos(\phi_n(t))$ is analytic, for all n, or equivalently[7] that the low frequency content of the n-th partial is in the amplitude $a_n(t)$, and that the high frequency content of the n-th partial is in the term $\cos(\phi_n(t))$.

1. *Amplitude modulation modeling*

Only the permanent regime is studied in this paper. Consequently, the expression of the amplitude modulation $a_n(t)$ we consider in this paper is such that

$$a_n(t) = \gamma_n \left(A_0 + \sum_{k=1}^{N_v} A_k \cos(2\pi k F_m t + \psi_k) \right), \tag{2}$$

for $n \in [1, N_h]$, where γ_n is the weight in amplitude modulation of n-th partial, where N_v is the number of harmonics of the vibrato frequency F_m, and where the parameters A_k and ψ_k of the Fourier series have to be estimated. We note in the following (by supposing $A_0 \neq 0$)

$$\alpha_k = \frac{A_k}{A_0} \tag{3}$$

the amplitude modulation rate of vibrato harmonic k, $\forall k \in [1, N_v]$. Two typical amplitude modulations are shown in Fig. 1, a pure sine amplitude modulation (case (a) : sine vibrato) and a flat amplitude signal (case (b) : no vibrato).

2. *Frequency modulation modeling*

On the other hand, we suppose that the instantaneous phase of the permanent regime expresses as

$$\phi_n(t) = 2\pi n F_s t + \sum_{l=1}^{N_v} \frac{n\beta_l F_s}{l F_m} \cos\left(2\pi l F_m t + \chi_{nl}\right), \tag{4}$$

where F_s is the playing frequency, where β_l and χ_{nl} are respectively the vibrato rate and the phase of vibrato harmonic l. An instantaneous frequency is associated to the n-th partial, defined as[7]

$$f_i^{(n)}(t) = \frac{1}{2\pi}\frac{d\phi_n(t)}{dt}. \tag{5}$$

Inserting (5) into (4) yields

$$f_i^{(n)}(t) = nF_s\left(1 - \sum_{l=1}^{N_v} \beta_l \, \sin(2\pi l F_m t + \chi_{nl})\right). \tag{6}$$

Independently of Fig. 1, two examples of frequency modulation are shown in Fig. 2 : a pure sine frequency modulation (case (a) : sine vibrato), and a flat one (case (b) : no vibrato).

3. *Assumptions and parameters to be estimated*

In the paper, only the permanent regime is studied. It is furthermore supposed that there is no recovery of instantaneous frequency from partial n to partial $n+1$ (see for example Fig. 2). This leads that the maximum value of instantaneous frequency of the n-th partial is largely inferior to the minimum value of instantaneous frequency of the (n+1)-th partial. Firstly, the maximum of instantaneous frequency of the n-th partial is bounded (upper limit) by

$$\text{Max}\left(f_i^{(n)}(t)\right) = nF_s\left(1 + \sum_{l=1}^{N_v} \beta_l\right), \tag{7}$$

and secondly, the minimum of instantaneous frequency of the (n+1)-th partial is bounded (lower limit) by

$$\text{Min}\left(f_i^{(n+1)}(t)\right) = (n+1)F_s\left(1 - \sum_{l=1}^{N_v} \beta_l\right). \tag{8}$$

As a consequence, there is no recovery of instantaneous frequency from partial n to partial $n+1$ if

$$(2N_h + 1)\sum_{l=1}^{N_v} \beta_l << 1. \tag{9}$$

Lastly, we suppose that $A_0 \neq 0$.

In the case of simulation, the controlled parameters are the number of vibrato harmonics N_v, the number of playing frequency vibrato harmonics N_h, and the sampling frequency f_e. The parameters to be estimated are the vibrato frequency F_m, the playing frequency F_s, the amplitude modulation parameters α_k (vibrato extent), ψ_k, the frequency modulation parameters β_l (vibrato rate), γ_n and χ_{nk}, for $n \in [1, N_h]$, and for $k, l \in [1, N_v]$. In this study, we focus on the estimation of F_m, F_s, α_k and β_l, for $k, l \in [1, N_v]$.

B. Amplitude modulation and instantaneous frequency estimations

Instantaneous amplitude and frequency concepts were originally developed in the theory of modulation in communications. These time-varying parameters are important features to estimate for many applications such as radar, sonar or seismology. Their estimations allow in particular to locate the time-varying frequency content of the signal. Many algorithms were developed to estimate these features and a tutorial review[8,9] was published in 1992. In the present paper, we use the envelop detection algorithm for estimating the amplitude modulation $a_n(t)$ (Eq. 2) and time-frequency distributions to estimate the instantaneous frequency $f_i^{(n)}(t)$ (Eq. 6).

1. *Amplitude modulation estimation*

In order to estimate the amplitude modulation, we demodulate firstly the signal $s(t)$ by means of a quadratic envelope detector. The principle of this detector is as follows : the signal is squared, before to be low-pass filtered. Then, by taking the square root of the low-pass filtered signal, we can obtained an estimation of the amplitude modulation[10]. The used filter is a Finite Impulse Response (FIR) digital filter, and its impulse response is calculated thanks to the Parks-McClellan algorithm[11]. Secondly, a synchronous detection is processed, in order to estimate A_k, F_m and ψ_k.

2. *Instantaneous frequency estimation*

Paraphrasing Cohen[7], "instantaneous frequency is one of the most intuitive concepts, since we are surrounded [...] by many phenomena whose periodicity changes". While instantaneous frequency seems to be a natural concept for describing our environment, its mathematical description is still an open question[7,8].

Furthermore, it has been shown[7,8] that instantaneous frequency may be related to time-frequency distributions (TFD). Indeed, such distributions allow to represent the frequency content of a signal as a joint function of time and frequency, and the instantaneous frequency may be then viewed as the average frequency at a given time.

Some distributions verify this property of local average (such as the Wigner-Ville distribution), while other TFD only approximate it (such as the spectrogram)[7,8]. Moreover, works have been done to construct a TFD which gives a perfect location of the instantaneous frequency[12]. In this paper, we use the spectrogram as an estimator of the instantaneous frequency. Once the instantaneous frequency is estimated, a synchronous detection is processed, in order to estimate β_l, F_m and χ_{nl} (for $l \in [1, N_v]$ and $n \in [1, N_h]$).

If the concept of instantaneous frequency is meaningful for a monocomponent signal, i.e. a signal where there is only one frequency varying with time for all time, a preliminary breakdown of the signal has to be done for a multicomponent signal. In the present case, we suppose that the instantaneous frequency of partials n and $(n+1)$ do not overlap (which is clearly the case for real-world vibrato signals). As a consequence, instantaneous frequency may be estimated for all the partials $n \in [1, N_h]$.

Following Cohen[2], we note $P_{SP}(t, f)$ the spectrogram of $s(t)$ according to

$$P_{SP}(t, f) = \left| \int s(t) h(\tau - t) e^{-j2\pi f \tau} \right|^2, \tag{10}$$

where $h(t)$ is a window function. In the following, we furthermore use the spectrogram to estimate the instantaneous frequency related to the n-th partial as above

$$\hat{f}_i^{(n)}(t) = \frac{\int_{B_n} f P_{SP}(t, f) df}{\int_{B_n} P_{SP}(t, f) df}, \tag{11}$$

where the partial n is related to the bandwidth B_n around the frequency nF_s. Even if $\hat{f}_i^{(n)}(t)$ is not a good estimator of the instantaneous frequency (due to an entanglement of signal and window[7]), narrowing the window $h(t)$ (or equivalently broadening the bandwidths B_n) allows to estimate correctly the instantaneous frequency[7], as shown in next section.

III. RESULTS AND DISCUSSION

A. Instantaneous amplitude and frequency estimators for test signals

Three test signals are simulated in this subsection, according to equations (1-6), for $N_h = 1$ and for three harmonics of the vibrato frequency ($N_v = 3$). The values of the parameters A_0, f_s, f_m, α_k and β_l are given in tables 1-3 (for k and $l \in [1,3]$), corresponding to realistic values of real-world vibratos.

We note in the following the levels of the vibrato strength from 1 (no vibrato) to 5 (exaggerated vibrato). In Table 1, the level of the vibrato strength is 2, with a low modulation rate in both amplitude and frequency. In Table 2, the level of the vibrato strength is 4, with a high modulation rate in both amplitude and frequency. Finally, the level of the vibrato strength in Table 3 is 4, with a low modulation rate in frequency and a high modulation rate in frequency. Furthermore, the rate of harmonic distorsion (HD) for the amplitude modulation express as

$$\mathrm{HD}_\alpha = \sqrt{\frac{\sum_{k=2}^{N_v} \alpha_k^2}{\sum_{k=1}^{N_v} \alpha_k^2}}. \tag{12}$$

For the frequency modulation, the rate of harmonic distorsion will be

$$\mathrm{HD}_\beta = \sqrt{\frac{\sum_{l=2}^{N_v} \beta_l^2}{\sum_{l=1}^{N_v} \beta_l^2}}. \tag{13}$$

We also estimate the spectral gravity center (SGC) according to

$$\mathrm{SGC}_\alpha = \frac{\sum_{k=1}^{N_v} k\alpha_k}{\sum_{k=1}^{N_v} \alpha_k}, \tag{14}$$

for the amplitude modulation, and

$$\mathrm{SGC}_\beta = \frac{\sum_{l=1}^{N_v} l\beta_l}{\sum_{l=1}^{N_v} \beta_l}, \tag{15}$$

for the frequency modulation.

The values of the estimated parameters and the associated errors given in Tables 1-3 show a good agreement between the simulations and the estimations. The associated errors for the estimation of α_1 are less than 1%, while the associated errors for the estimation of β_1 are less than 5%. Furthermore, the playing frequency F_s and the vibrato frequency F_m are respectively estimated with errors less than 0.1% and 2%. Even if the values of β_3 and α_3 are poorly estimated, due to the very weak values of the simulated parameters, we maintain that the signal processing methods described in section II are well-suited for the analysis of vibratos. Lastly, the harmonic distorsion rate is better estimated for the amplitude modulation than for the frequency modulation.

B. Real-world signals, estimation of parameters and discussion

In order to apply the signal processing methods on real sounds, the saxophone player Christophe Bois has recorded self-sustained notes, from which one second of the permanent regime is selected and analysed. The database contains 21 samples which are summarised in Table 4. The database has been filled by playing the note E3, at two nuances, piano and forte, at five vibrato strength levels, from soft (1) to high (5), using the two kinds of vibrato, "a la machoire" and "sur l'air". A class of records has been set from 2 to 11. A same class of record is corresponding to the same note, the same nuance and the same vibrato strength level, the way of playing being "a la machoire" or "sur l'air". Most of the possibilities have been explored, giving the 21 samples. The samples have been analysed using the signal processing methods described in chapter II in order to extract the parameters α_k representative of the amplitude modulation, and β_l representative of the frequency modulation. The first coefficients β_1 as a function of α_1 are displayed figure 3. Having a look on figure 3, no obvious conclusion can be drawn, the two kinds of vibratos can not be separated by their (α_1, β_1) values. Even if two samples having a close pair value (α_1, β_1) on figure 3 can be easily distinguished by an informal listening test. A first result is that the kind of vibrato is not directly linked with a kind of signal modulation. An other cœfficient has then to be find. As explained previously in section IIIA, harmonic distorsion rates can be computed from the higher coefficients α_k and β_l (for $k, l > 1$) of the real signals. The rate of harmonic distorsion for the amplitude modulation (figure 4) and for the frequency modulation (figure 5) are estimated successively from the real signals as a function of the class of record. Notice that the two ways of playing vibrato are quite well separated : the vibratos "a la machoire" do exhibit higher values of the amplitude modulation distorsion than the vibratos "sur l'air" (figure 4). At the opposite, the vibratos "a la machoire" do exhibit lower values of the frequency modulation distorsion than the vibratos "sur l'air" (figure 5). Nevertheless, the separation is not exclusive. For each of the two distorsion rates, there is a counter-example corresponding to a high pronounced vibrato at forte nuance (record numbers 10 and 21 on figure 4), and to a high pronounced vibrato at piano nuance (record numbers 5 and 16 on figure 5). As an alternative of the distorsion rate, a spectral gravity center of the vibrato modulation can be defined. The corresponding results associated to amplitude modulation are displayed in figure 6. Theses conclusions are the same than the ones drawn from the distorsion rate (figure 4), but there is no counter-example anymore, and the two ways of vibrato playing are well separated then. Notice that several samples corresponding to other notes than E3, E4 for example, have been recorded and analysed. The results obtained are compatible with the conclusions drawn from the E3 note's extensive study.

The algorithm of both amplitude and frequency modulation estimations is also applied to signals coming from playing performance. The database is made up of extracts of several recordings, where only the vibrato of the saxophonist is present. The selected musical tunes are presented in table 5. In figure 3, the estimations of α_1 and β_1 are compared with the estimations of the vibratos of self-sustained notes. Moreover, we compare the estimations of HD_α (figure 4), HD_β (figure 5), SGC_α (figure 6) and SGC_β (figure 7), for these signals coming from playing performance, with the cases of self-sustained notes vibratos. We call class 12 the class associated with the signals coming from playing performance.

Figures 3 to 7 show how the estimated parameters of the signals coming from playing performance (class number 12) are coherent with the values of the database of real-world signals. For the record number 242 (Table 5), note that the harmonic distorsion rate HD_α (Fig. 4) is about 70%. Parameter values of α_1, β_1, HD_α, HD_β, SGC_α and SGC_β are clearly in the same area of the corresponding parameters for self-sustained notes.

C. Simulated signals

1. *Physical modeling*

The nature of the sound production of single reed instruments is now well understood[13]. Using an elementary model for the reed and the mouthpiece, coupled with an idealized instrument, a saxophone here, a large range of the musical behaviour of the single reed instruments is described. The elementary model is based on two equations : one for the non-linear excitation mechanism, the reed-mouthpiece system (Eq. 16) and the one for the resonator, regarded as a linear system (Eq. 17). The two equations make the coupling between the two following variables : $u(t)$, the volume flow entering into the instrument, and $p(t)$, the acoustical pressure in the mouthpiece

$$\begin{cases} u(t) = wH_O\left(1 - \frac{p_m - p(t)}{P_M}\right)\mathrm{sign}\left(p_m - p(t)\right)\sqrt{\frac{2|p_m - p(t)|}{\rho}} \quad \text{if} \quad p_m - p(t) \leq P_M \\ u(t) = 0 \quad \text{if} \quad p_m - p(t) \geq P_M \end{cases}, \tag{16}$$

$$p(t) = \rho c u(t) + r(t) * \left(p(t) + \rho c u(t)\right), \tag{17}$$

where w is the effective width of the reed channel, H_0 the reed opening at rest, p_m the mouth pressure, ρ the air density and c the sped of sound in free space. The limit value P_M for which the reed closes the opening is given by $P_M = kH_0$ where k is the reed stiffness. P_M is the minimum value of the mouth pressure above which the static solution corresponding to the reed blocked against the lay is stable. The reflection function $r(t)$ of the pipe is obtained by inverse

Fourier transform of the reflection coefficient $R(j\omega)$ defined as a function of the dimensionless input impedance $Z(j\omega)$

$$R(j\omega) = \frac{Z(j\omega) - 1}{Z(j\omega) + 1}. \tag{18}$$

The saxophone bore is mainly conical. An approximation of the truncated cone by using a system of two cylinders can be used. Their lengths L_b and L_a respectively, are equal to the lengths of the truncated cone and of the truncature respectively. Typically the ratio L_a/L_b has been choosen to be equal to 5. The dimensionless input impedance $Z(j\omega)$ is defined as follows[14]

$$\frac{1}{Z(j\omega)} = \frac{1}{\mathrm{th}(\Gamma L_a)} + \frac{1}{\mathrm{th}(\Gamma L_b)}, \tag{19}$$

where Γ is the propagation constant taken into account the visco-thermal effects (losses and dispersion).

In order to get oscillations a simulation technique in discrete time-domain is used[15,16]. Assuming the control parameters (P_m, H_0, k) to be constant, periodic oscillations are obtained in permanent regimes after a short transient. A way to reproduce vibratos by simulations is to use control parameters slowly varying slowly in time. Typically, simulations have been done using control parameters varying harmonically at 5Hz.

2. *Estimation of parameters and discussion*

A set of simulations corresponding to each one of the two control parameters P_m, and H_0 have been done. The modulation rate of each parameter is equal to 5 Hz. The modulation extent of P_m, and H_0 is varying from 5% to 30%, and from 10% to 40% respectively, of their mean value. Three sets of simulations have been calculated : one set corresponding to a variation of H_0, an other one to a variation of P_m, the third one corresponding to a modulation of both the control parameters. Then the simulated signals have been analysed in the same way than the real sounds by using the signal processing methods described in section II in order to evaluate the values of α_1 and β_1. The results are shown in Fig. 8 and Fig. 9 using the same kind of display than those of real sounds given chapter III.B.

The preliminary results of Fig. 8 show that the mouth pressure P_m mainly controls the amplitude modulation. And the reed opening H_0 mainly controls the frequency modulation. But each control parameter does influence both the amplitude and frequency modulations significantly. The results displayed in Fig. 8 do not show any separation between each of the three sets of simulations. At the opposite, the SGC results applied to amplitude modulation (Fig. 9) seems to be able to separate the set of H_0 variations simulations, and the set of P_m variations simulations. According to our hypotheses assuming that the vibrato "a la machoire" is linked with a H_0 variation, and the vibrato "sur l'air" with a P_m variation, then the two kinds of vibratos are separated quite successfully.

IV. CONCLUDING REMARKS

In this paper some alto saxophones instruments vibratos have been studied. Suitable signal processing methods have been developed in order to estimate parameters of amplitude and frequency modulations. First the methods have been validated for test signals, and then they have been applied to the real saxophone vibrato sounds, and to simulated vibrato sounds coming from physical modelling of saxophone-like instruments. The methods are able to estimate the characteristics of the vibrato oscillations by extracting the first harmonics of the periodic vibrato oscillation, the vibrato extent and the vibrato rate, with errors less than 5%. On one hand the harmonic components of the real vibrato sounds have been extracted, and no straightforward difference between the two techniques of playing vibrato, "a la machoire" and "sur l'air", have been shown directly from these components. On the other hand, it has been shown that the two techniques can be separated by using a cœfficient representing the vibrato amplitude distortion, like a spectral gravity center. In parallel, simulations based on control parameters slow modulations have been analysed. According to our hypotheses assuming that the vibrato "a la machoire" is linked to a H_0 variation, and the vibrato "sur l'air" to a P_m variation, then the two kinds of vibrato techniques have been roughly simulated. If vibratos of singing voices are mainly linked to frequency modulation, significant amplitude modulations have been extracted from saxophone vibratos. Further studies might be done on other wind instruments vibratos. An important work has to be produced on players in order to extract direct information on the slowly varying control parameters. If it seems easy to extract the mouth pressure modulation, to get the opening reed-lay modulation during the performance technique seems to be a hard task.

ACKNOWLEDGMENTS

The authors would like to express gratitude to the professional saxophone players Christophe Bois and Gregory Letombe for helpful discussions and for providing vibrato database. The help of Pierre Couratier at the beginning of the project is acknowledged too.

Références

[1] E. Prame, "Measurements of the vibrato rate of ten singers," J. Acoust. Soc. Am. **96**(4), 1979-1984 (1994).

[2] E. Prame, "Vibrato extent and intonation in professional western lyric singing," J. Acoust. Soc. Am. **102**(1), 616-621 (1997).

[3] I. Arroabarren, M. Zivanovic, J. Bretos, A. Ezcura & A. Carlosena, "Measurements of vibrato in lyric singers," IEEE Trans. Instrum. Meas. **51**(4), 660-665 (2002).

[4] J.C. Brown, "Frequency ratios of spectral components of musical sounds," J. Acoust. Soc. Am. **99**(2), 1210-1218 (1995).

[5] C. D'Allesandro & M. Castellengo, "The pitch of short-duration vibrato tones," J. Acoust. Soc. Am. **95**(3), 1617-1630 (1993).

[6] M. Mellody & G.H. Wakefield, "The time-frequency characteristics of violin vibrato : modal distribution analysis and synthesis," J. Acoust. Soc. Am. **107**(1), 598-611 (2000).

[7] L. Cohen, "Time Frequency Analysis," Prentice Hall PTR (1995).

[8] B. Boashash, "Estimating and interpreting the instantaneous frequency of a signal. Part 1 : Fundamentals," Proc. IEEE, **80**(4), 520-538 (1992).

[9] B. Boashash, "Estimating and interpreting the instantaneous frequency of a signal. Part 2 : Algorithms and applications," Proc. IEEE, **80**(4), 540-568 (1992).

[10] B.P. Lathi, "Modern digital and analog communications systems," Oxford University Press (1998).

[11] A.V. Oppenheim & R.W. Schafer, "Discrete-time signal processing," Prentice Hall Signal Processing Series, 2nd Edition (1999).

[12] C. Mellet, J.-C. Valière & V. Valeau, "Use of frequency trackers in Laser Doppler Velocimetry for sound field measurement : comparative study of two estimators," Mech. Sys. Sig. Proc. **17**(2), 329-344 (2003).

[13] J. Kergomard, "Elementary considerations on reed instrument oscillations", in Mechanics of Musical instruments, Hirschberg & al editors, 229-290 Springer (1995).

[14] S. Ollivier, J.-P. Dalmont & J. Kergomard, "Idealized models of reed instruments. Part I : analogy with the bowed string", ACUSTICA-Acta Acustica, In Press (2004).

[15] M. Atig, J.-P. Dalmont and J. Gilbert, "Saturation mechanism in clarinet-like instruments, the effect of the localized non-linear losses", Applied Acoustics, In Press (2004).

[16] B. Gazengel, J. Gilbert and N. Amir, "Time domain simulations of single reed wind instrument. From the measured input impedance to the synthesis signal. Where are the traps ?", Acta Acustica **3**, 445-472 (1995).

FIG. 1 - Test signals $s(t)$ (left panel) and associated amplitude modulations (right panel). (a) : amplitude modulation of a test signal (vibrato case) for the following set of parameters : $\alpha_1 = 3/7$, $\alpha_k = 0\ \forall k > 1$ (top row). (b) : amplitude modulation of a test signal (nonvibrato case) for the following set of parameters $A_0 = 1$, $\alpha_k = 0\ \forall k > 0$ (bottom row).

FIG. 2 - Instantaneous frequency of test signals. (a) : frequency modulation of a test signal (vibrato case) for the following set of parameters : $N_h = 3$, $N_v = 1$, $\beta_k = 0.1$ and $\beta_k = 0\ \forall k > 1$. (b) : frequency modulation of a test signal (nonvibrato case) for the following set of parameters : $N_h = 3$ and $\beta_k = 0\ \forall k$.

FIG. 3 - β_1 as a function of α_1. The associated record numbers are in Tables 4 and 5. Circles : Vibrato "a la machoire". Crosses : Vibrato "sur l'air". Diamonds : Vibrato coming from playing performance.

FIG. 4 - Harmonic distorsion cœfficient HD_α as a function of the class of record. Estimation from the amplitude modulation. The associated record numbers and the classes of records are in Tables 4 and 5. Circles : Vibrato "a la machoire". Crosses : Vibrato "sur l'air". Diamonds : Vibrato coming from playing performance arbitrarily associated to class 12.

FIG. 5 - Harmonic distorsion cœfficient HD_β as a function of the class of record. Estimation from the frequency modulation. The associated record numbers and the classes of records are in Tables 4 and 5. Circles : Vibrato "a la machoire". Crosses : Vibrato "sur l'air". Diamonds : Vibrato coming from playing performance arbitrarily associated to class 12.

FIG. 6 - Spectral gravity center SGC_α as a function of the class of record. Estimation from the amplitude modulation. The associated record numbers and the classes of records are in

Tables 4 and 5. Circles : Vibrato "a la machoire". Crosses : Vibrato "sur l'air". Diamonds : Vibrato coming from playing performance arbitrarily associated to class 12.

FIG. 7 - Spectral gravity center SGC_β as a function of the class of record. Estimation from the frequency modulation. The associated record numbers and the classes of records are in Tables 4 and 5. Circles : Vibrato "a la machoire". Crosses : Vibrato "sur l'air". Diamonds : Vibrato coming from playing performance arbitrarily associated to class 12.

FIG. 8 - β_1 as a function of α_1 (simulated signals).

FIG. 9 - Harmonic distorsion cœfficient as a function of arbitrary database signals (simulated signals) as a function of (a) H_0, (b) P_m.

FIG. 1

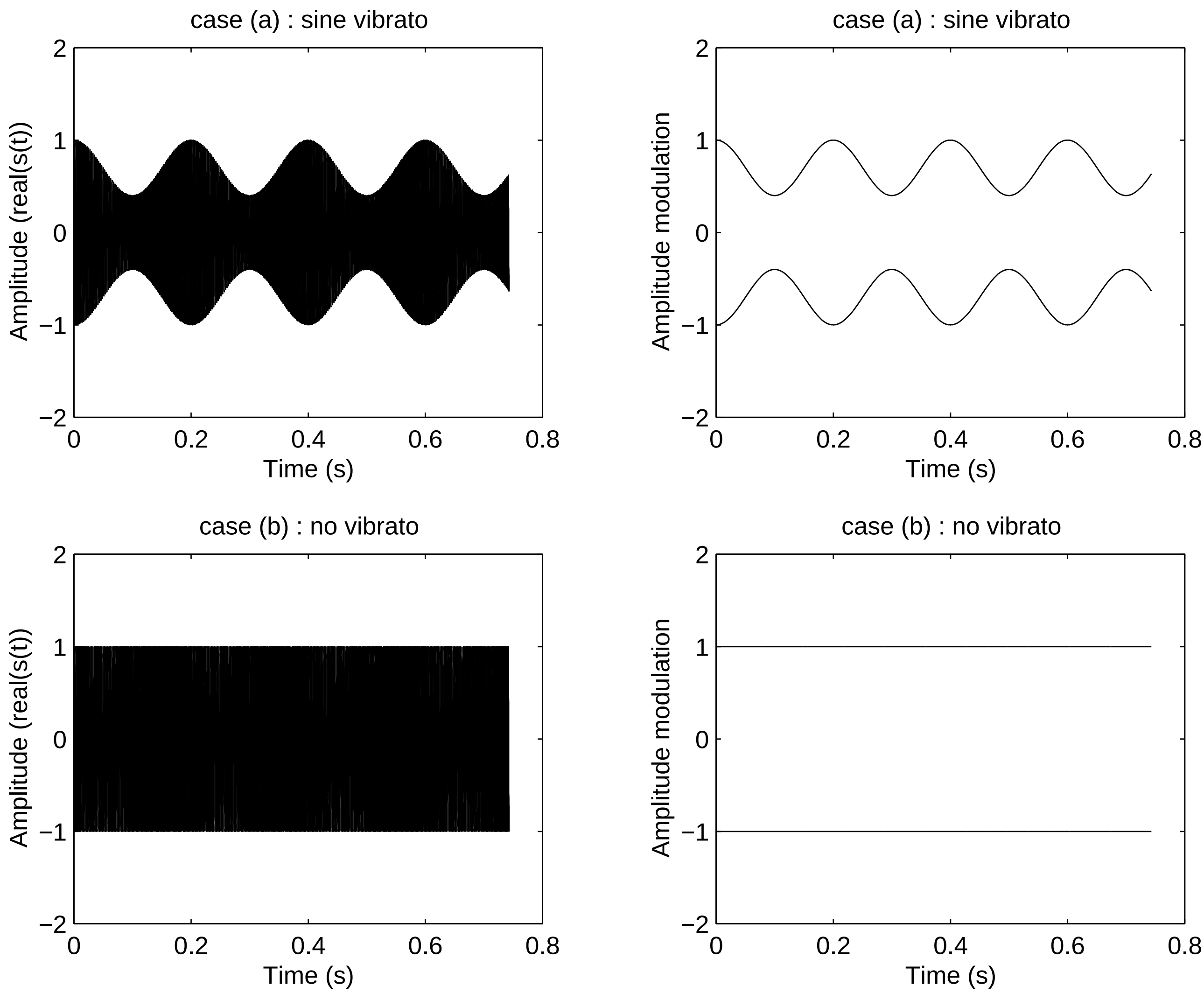
case (a) : sine vibrato
Amplitude (real(s(t))
Time (s)
case (a) : sine vibrato
Amplitude modulation
Time (s)
case (b) : no vibrato
Amplitude (real(s(t))
Time (s)
case (b) : no vibrato
Amplitude modulation
Time (s)
2
1
0
−1
−2
0
0.2
0.4
0.6
0.8

FIG. 2

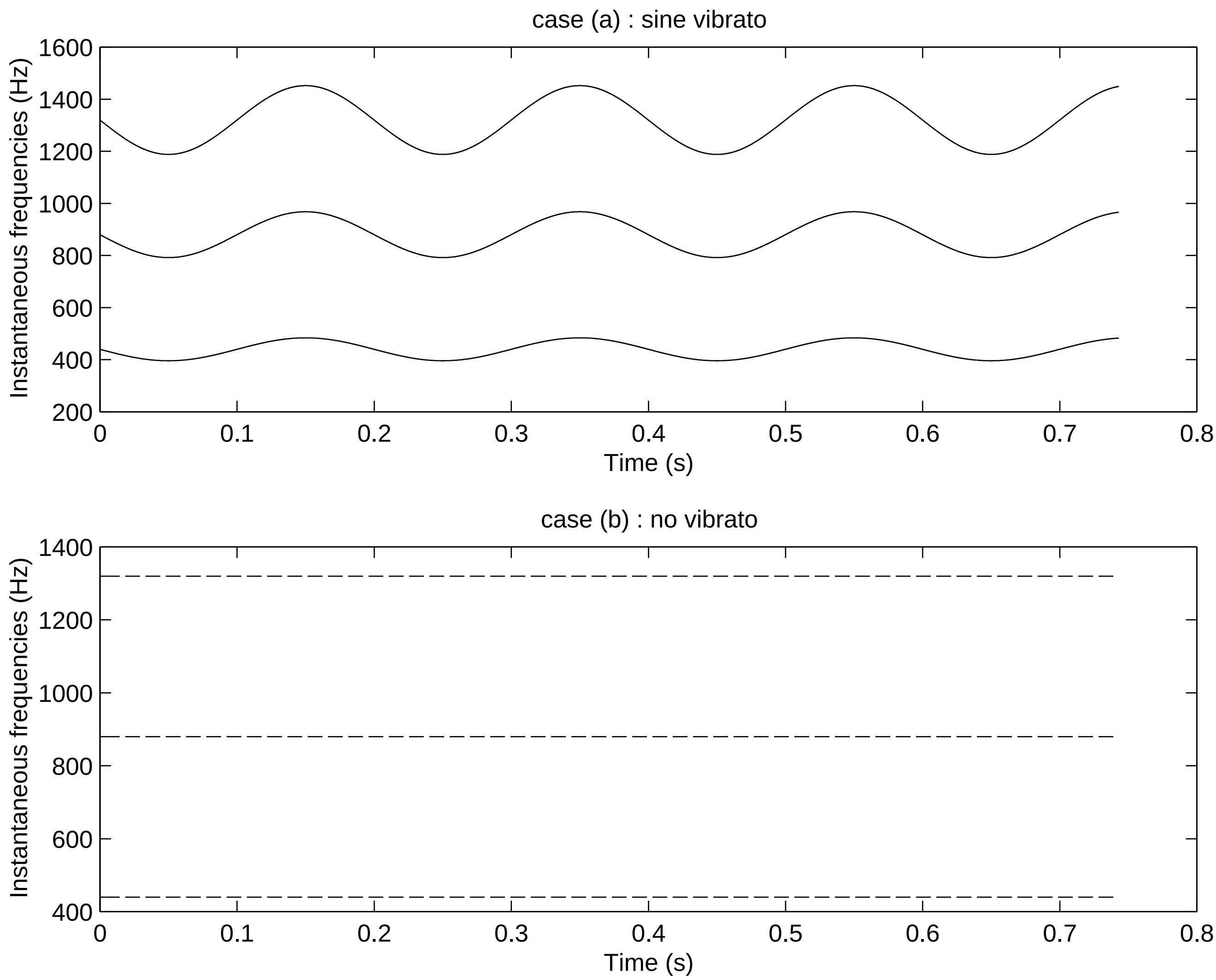
case (a) : sine vibrato
Instantaneous frequencies (Hz)
1600
1400
1200
1000
800
600
400
200
0
0.1
0.2
0.3
0.4
0.5
0.6
0.7
0.8
Time (s)
case (b) : no vibrato
Instantaneous frequencies (Hz)
1400
1200
1000
800
600
400
0
0.1
0.2
0.3
0.4
0.5
0.6
0.7
0.8
Time (s)

FIG. 3

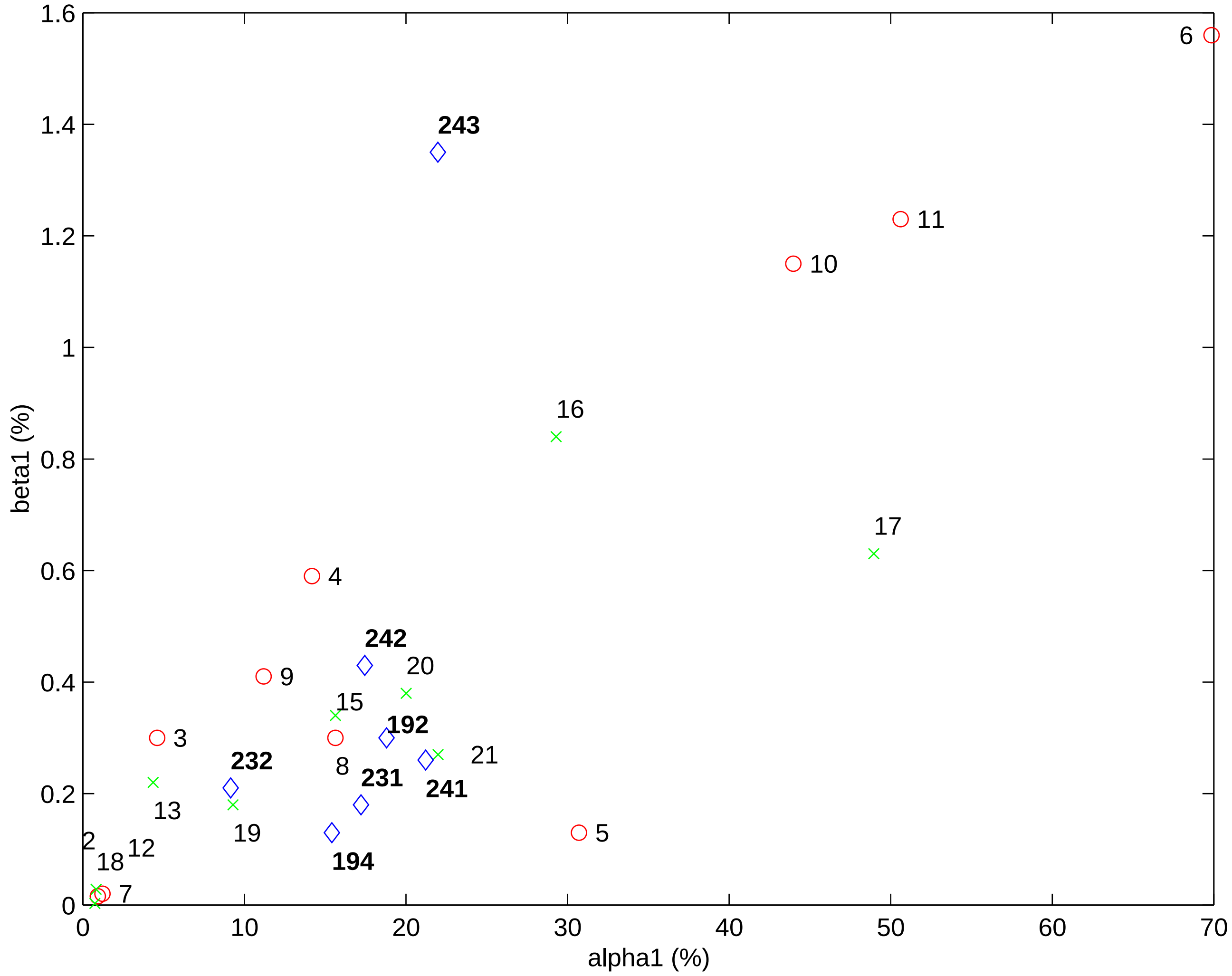

beta1 (%)
alpha1 (%)
0
0.2
0.4
0.6
0.8
1
1.2
1.4
1.6
0
10
20
30
40
50
60
70
6
243
11
10
16
17
4
242
20
9
15
192
3
232
8
231
21
241
13
19
5
2
18
12
194
7

FIG. 4

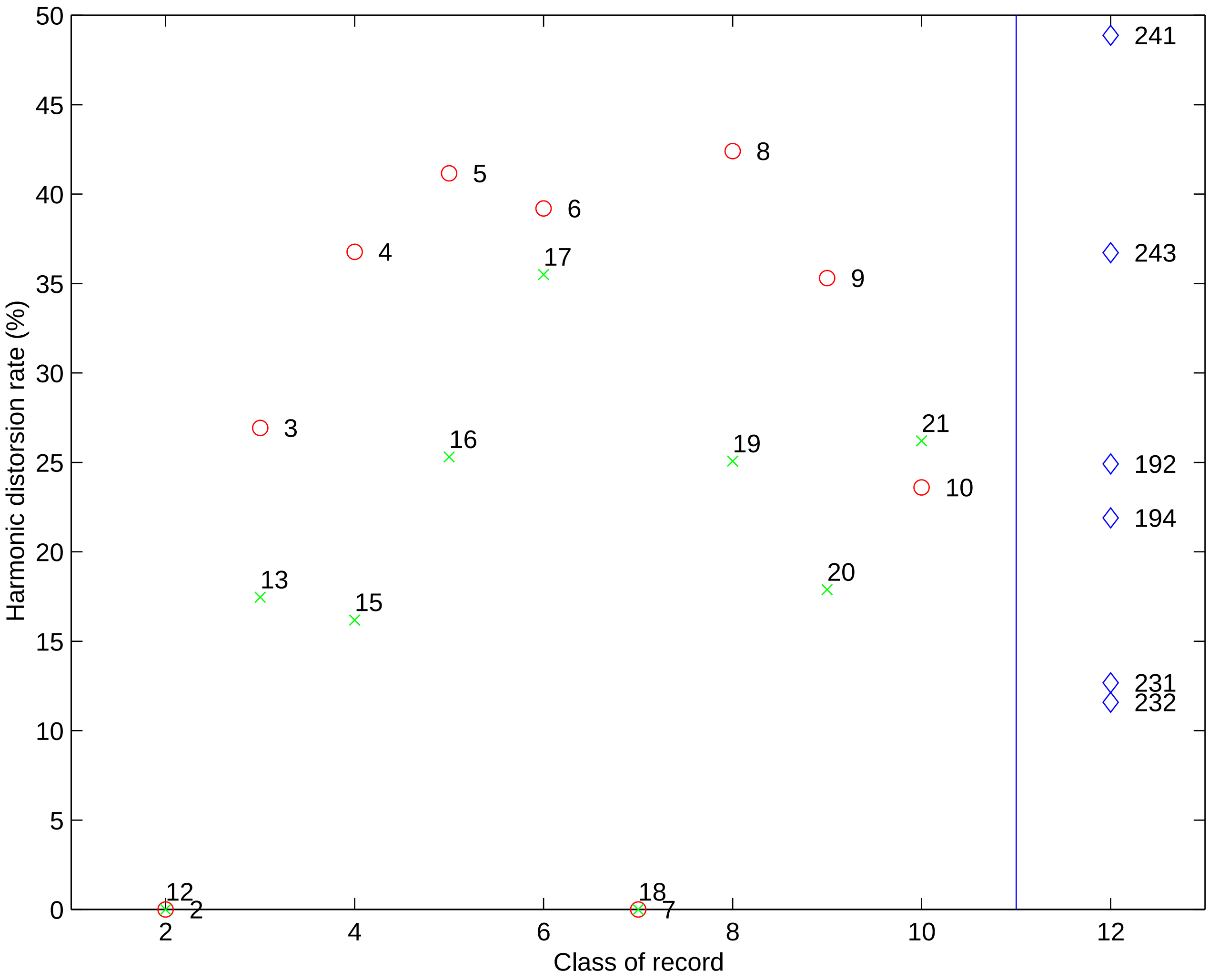

Harmonic distorsion rate (%)
Class of record
0
5
10
15
20
25
30
35
40
45
50
2
4
6
8
10
12
241
243
192
194
231
232
2
3
4
5
6
7
8
9
10
12
13
15
16
17
18
19
20
21

FIG. 5

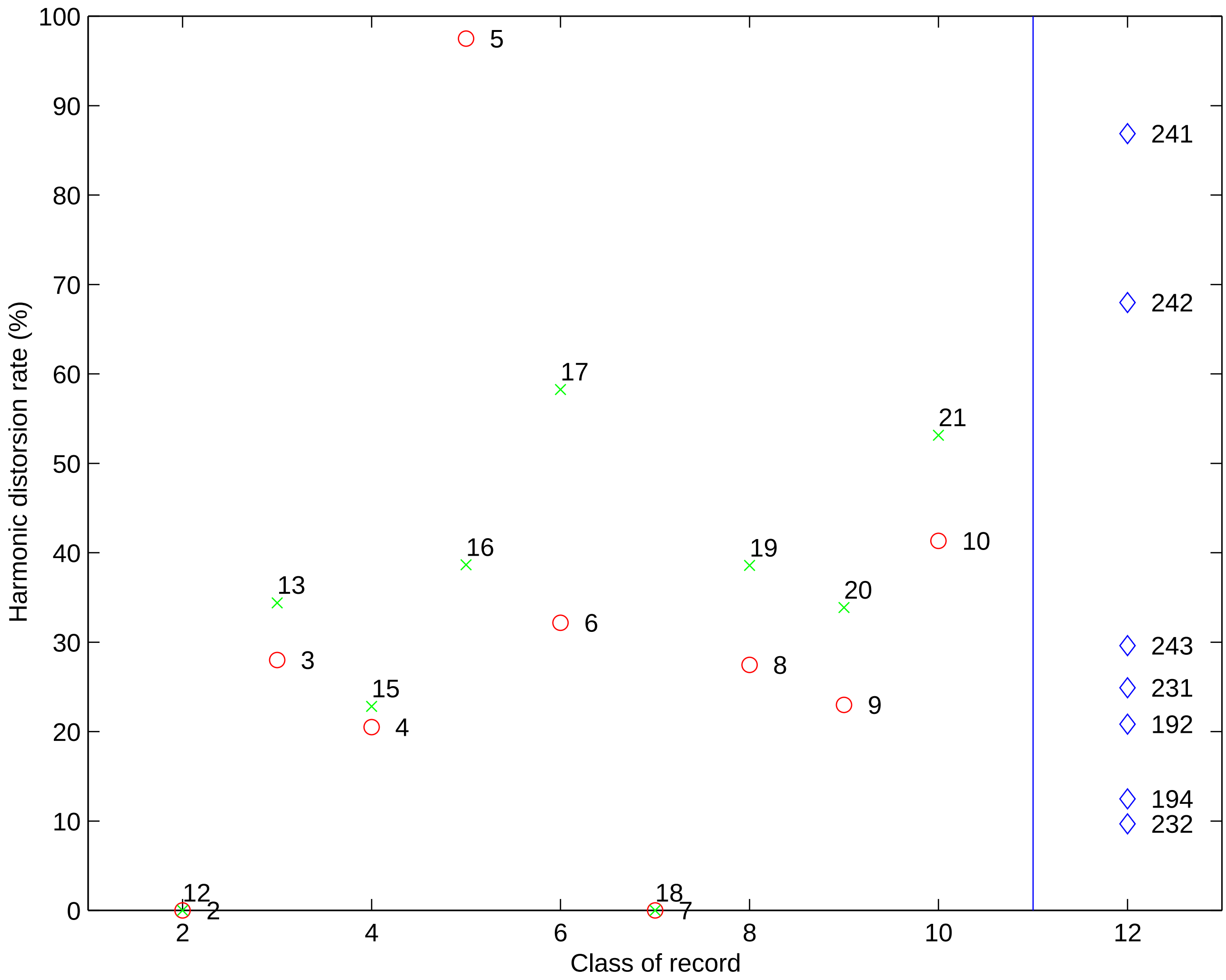
Harmonic distorsion rate (%)
Class of record
0
10
20
30
40
50
60
70
80
90
100
2
4
6
8
10
12
5
241
242
17
21
16
19
10
13
20
6
3
8
243
15
231
4
9
192
194
232
12
2
18
7

FIG. 6

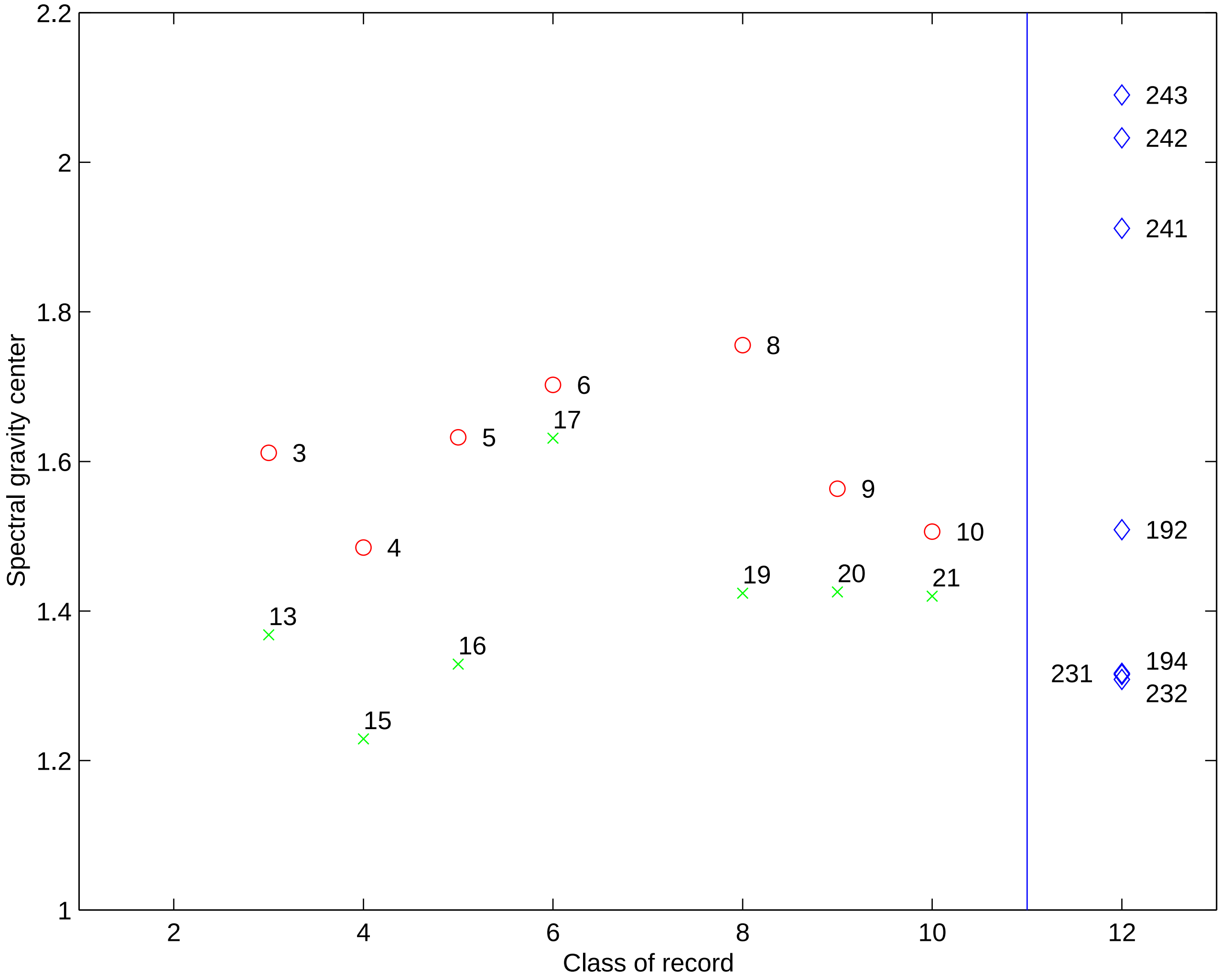

Spectral gravity center
Class of record
2.2
2
1.8
1.6
1.4
1.2
1
2
4
6
8
10
12
243
242
241
8
6
17
3
5
9
10
192
4
19
20
21
13
16
231
194
232
15

FIG. 7

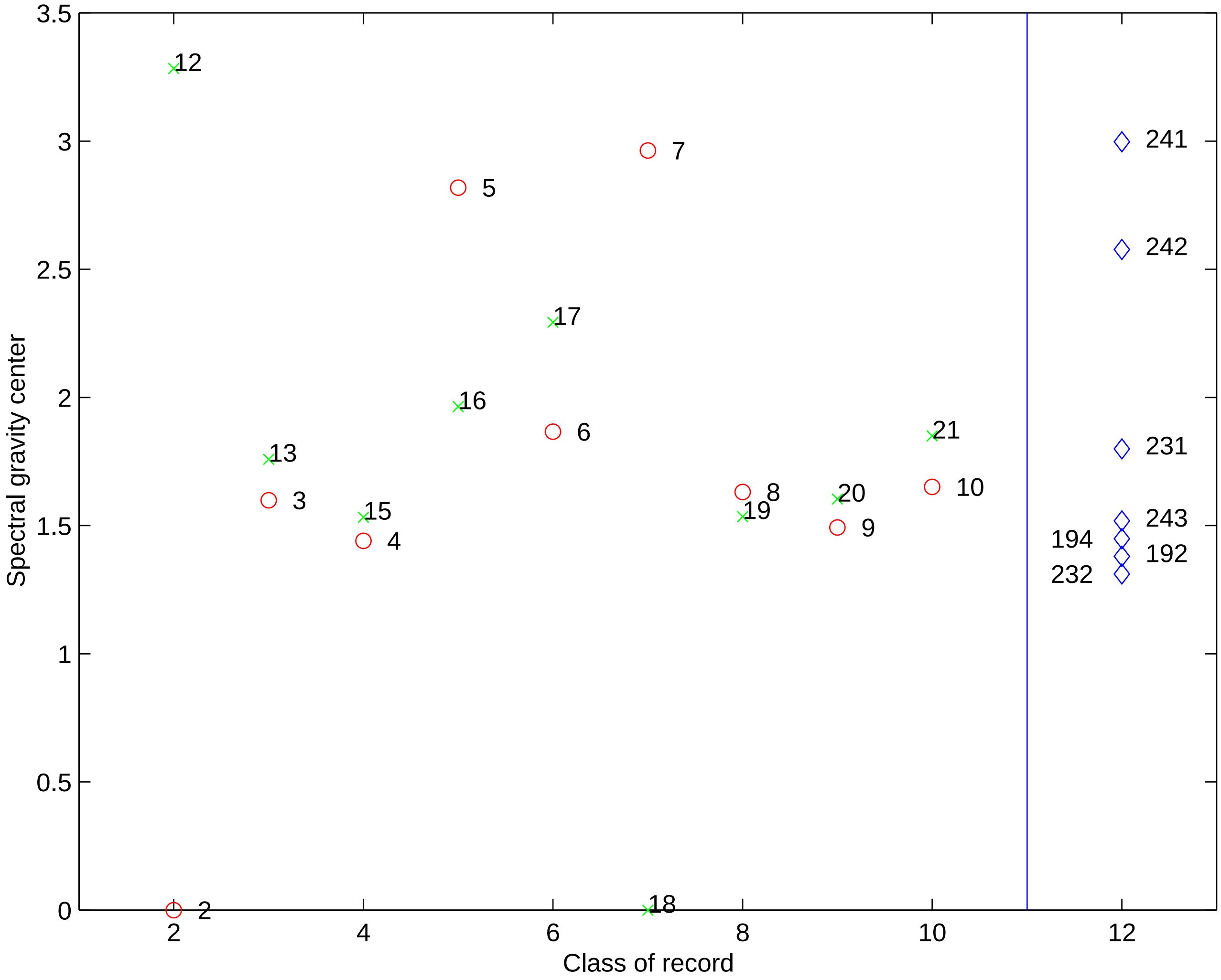
Spectral gravity center
Class of record
3.5
3
2.5
2
1.5
1
0.5
0
2
4
6
8
10
12
12
13
15
16
17
18
19
20
21
2
3
4
5
6
7
8
9
10
241
242
231
243
194
192
232

FIG. 8

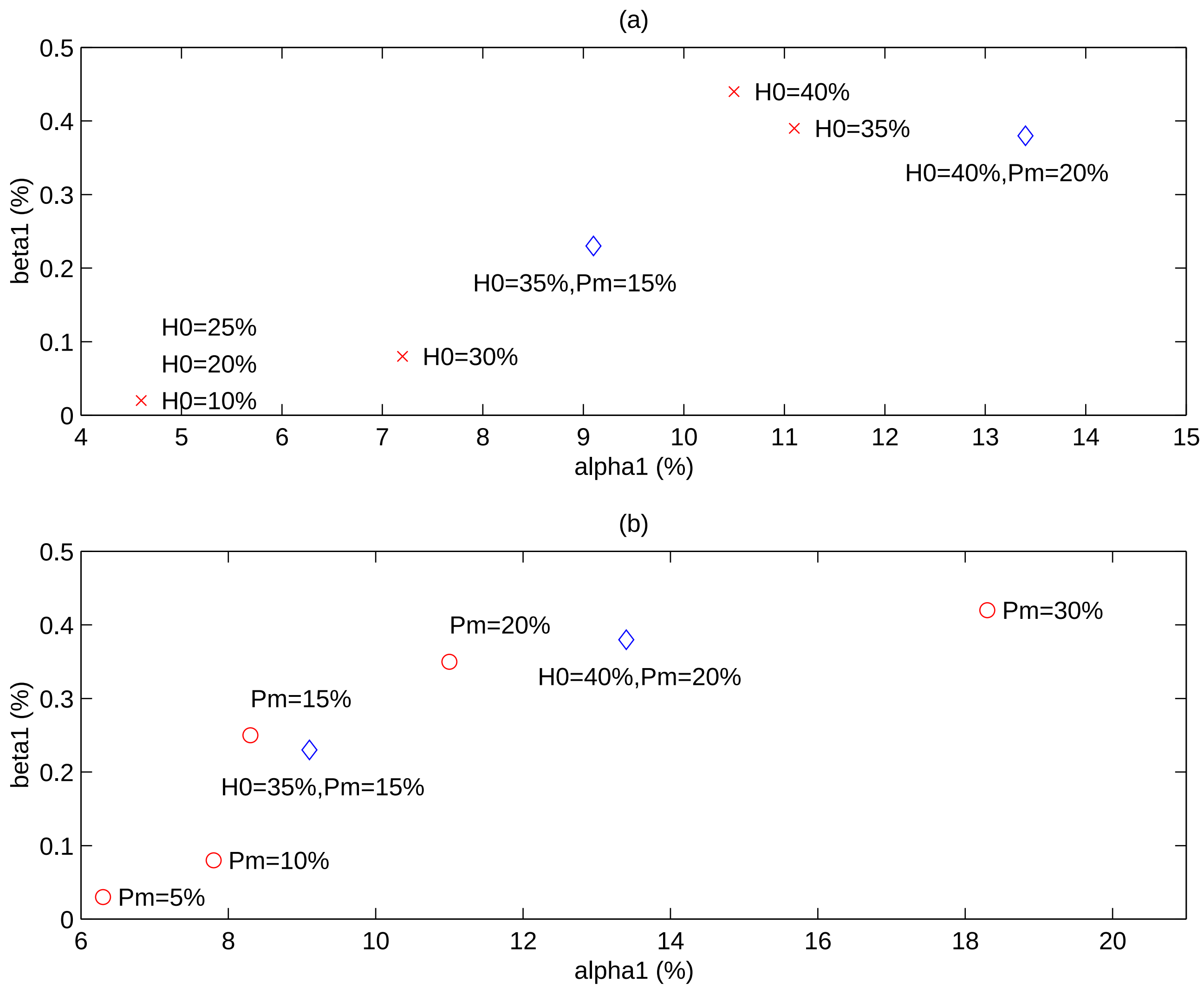
(a)
beta1 (%)
alpha1 (%)
H0=40%
H0=35%
H0=40%,Pm=20%
H0=35%,Pm=15%
H0=25%
H0=20%
H0=10%
H0=30%
(b)
beta1 (%)
alpha1 (%)
Pm=30%
Pm=20%
H0=40%,Pm=20%
Pm=15%
H0=35%,Pm=15%
Pm=10%
Pm=5%

FIG. 9

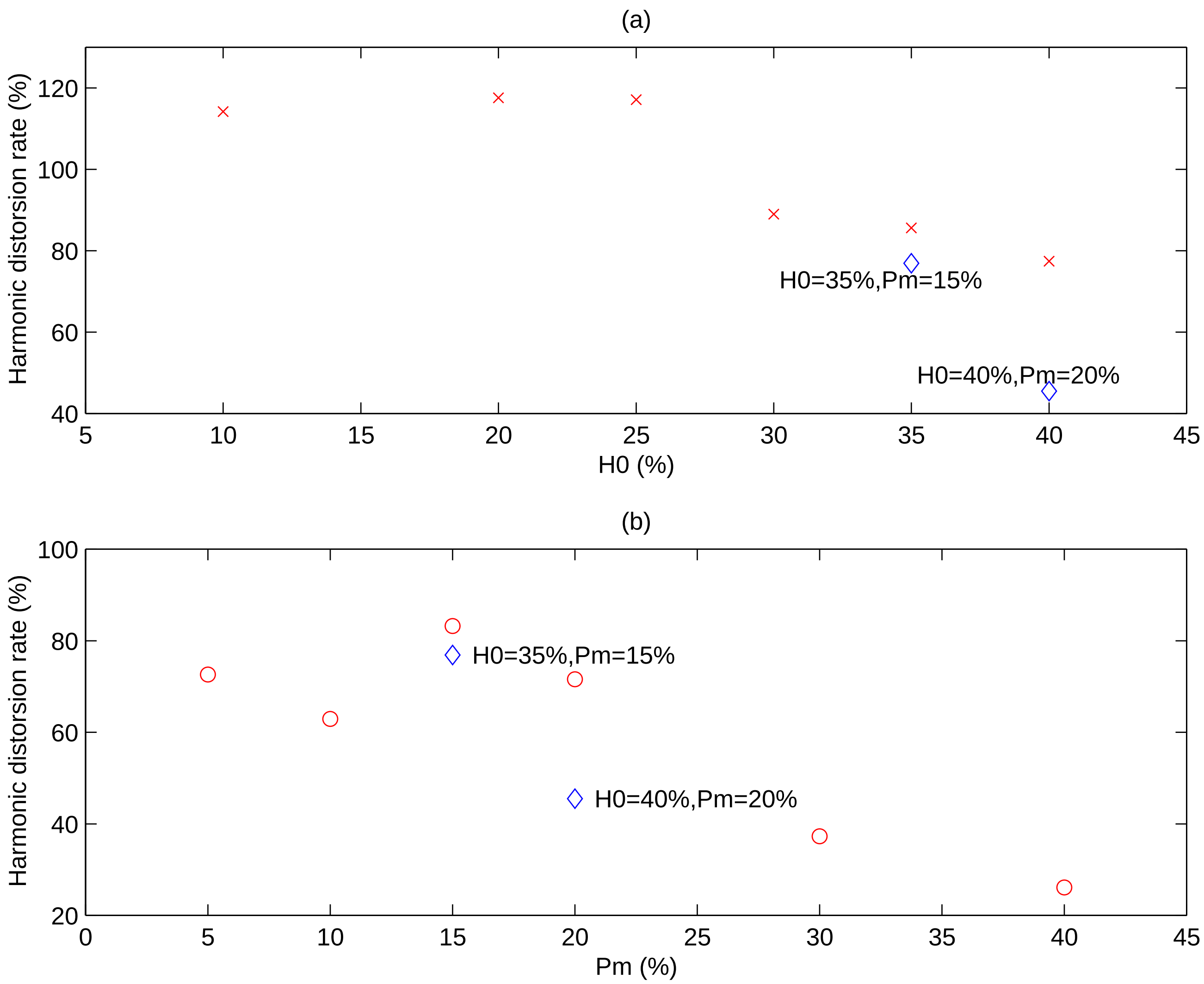
(a)
Harmonic distorsion rate (%)
120
100
80
60
40
5
10
15
20
25
30
35
40
45
H0 (%)
H0=35%,Pm=15%
H0=40%,Pm=20%
(b)
Harmonic distorsion rate (%)
100
80
60
40
20
0
5
10
15
20
25
30
35
40
45
Pm (%)
H0=35%,Pm=15%
H0=40%,Pm=20%

TAB. 1 - First set of parameters of a test signal. Simulated values, estimated values and associated errors.

TAB. 2 - Second set of parameters of a test signal. Simulated values, estimated values and associated errors.

TAB. 3 - Third set of parameters of a test signal. Simulated values, estimated values and associated errors.

TAB. 4 - Database of real signals. Record number, vibrato strength (from 1 : no vibrato, to 5 : exaggerated vibrato), nuance, kind of vibrato and class of record.

TAB. 5 - Database of signals coming from playing performance. Record number, title of musical tune, nearest note (E3 or E4), vibrato strength (from 1 : no vibrato, to 5 : exaggerated vibrato). The class associated to these signals is class 12.

TABLE 1

Parameter	Simulated value	Estimated value	Associated error (%)
A_0 (Eq. 2)	0.34	0.366	7.6
F_s (Hz)	392	391.98	< 0.1
F_m (Hz)	4.5	4.44	1.3
α_1 (Eq. 3)	0.441	0.443	0.45
α_2 (Eq. 3)	0.176	0.175	0.56
α_3 (Eq. 3)	0.029	0.033	0.45
β_1 (Eq. 6)	0.006	0.0061	1.7
β_2 (Eq. 6)	0.003	0.0027	10
β_3 (Eq. 6)	0.002	0.0015	25
HD_α (Eq. 12)	0.375	0.373	0.53
HD_β (Eq. 13)	0.515	0.452	12.23
SGC_α (Eq. 14)	1.362	1.37	0.6
SGC_β (Eq. 15)	1.636	1.553	5.07

TABLE 2

Parameter	Simulated value	Estimated value	Associated error (%)
A_0 (Eq. 2)	0.4	0.435	8.7
F_s (Hz)	392	391.97	< 0.1
F_m (Hz)	5	4.95	1
α_1 (Eq. 3)	0.75	0.745	0.67
α_2 (Eq. 3)	0.25	0.244	2.4
α_3 (Eq. 3)	0.125	0.106	15.2
β_1 (Eq. 6)	0.01	0.0102	2
β_2 (Eq. 6)	0.004	0.0038	5
β_3 (Eq. 6)	0.004	0.0027	32.5
HD_α (Eq. 12)	0.349	0.336	3.7
HD_β (Eq. 13)	0.492	0.416	15.45
SGC_α (Eq. 14)	1.362	1.37	0.6
SGC_β (Eq. 15)	1.636	1.553	5.07

TABLE 3

Parameter	Simulated value	Estimated value	Associated error (%)
A_0 (Eq. 2)	0.3	0.326	8.7
F_s (Hz)	1590	1590.1	$<$0.1
F_m (Hz)	4.75	4.66	1.9
α_1 (Eq. 3)	0.7	0.696	0.57
α_2 (Eq. 3)	0.3	0.296	1.33
α_3 (Eq. 3)	0.067	0.059	11.94
β_1 (Eq. 6)	0.002	0.0021	5
β_2 (Eq. 6)	0.0015	0.00153	2
β_3 (Eq. 6)	0.002	0.0015	25
HD_α (Eq. 12)	0.402	0.398	1
HD_β (Eq. 13)	0.781	0.714	8.6
SGC_α (Eq. 14)	1.407	1.394	0.92
SGC_β (Eq. 15)	2	1.88	5

Tab. 4

Record number	Vibrato strength [1-5]	Nuance	Kind of Vibrato	Class of record
2	1	piano	a la machoire	**2**
3	2	piano	a la machoire	**3**
4	3	piano	a la machoire	**4**
5	4	piano	a la machoire	**5**
6	5	piano	a la machoire	**6**
7	1	forte	a la machoire	**7**
8	2	forte	a la machoire	**8**
9	3	forte	a la machoire	**9**
10	4	forte	a la machoire	**10**
11	5	forte	a la machoire	**11**
12	1	piano	sur l'air	**2**
13	2	piano	sur l'air	**3**
15	3	piano	sur l'air	**4**
16	4	piano	sur l'air	**5**
17	5	piano	sur l'air	**6**
18	1	forte	sur l'air	**7**
19	2	forte	sur l'air	**8**
20	3	forte	sur l'air	**9**
21	4	forte	sur l'air	**10**

TAB. 5

Record number	Title of musical tune	Nearest note	Vibrato strength
192	*Syrinx* of C.Debussy, played by F.Chouraki	E4	3-4
194	*Syrinx* of C.Debussy, played by F.Chouraki	E4	1-2
231	*Quatuor* of Olav Berg, played by H.Bergersens	E3	2-3
232	*Quatuor* of Olav Berg, played by H.Bergersens	E3	2-3
241	*An der schőnen blauen Donau* of J.Strauss, by Spike Jones	E3	4-5
242	*An der schőnen blauen Donau* of J.Strauss, by Spike Jones	E3	4-5
243	*An der schőnen blauen Donau* of J.Strauss, by Spike Jones	E3	5